# Ultracold collisions in metastable helium

**G Peach[1], D G Cocks[2] and I B Whittingham[2]**

[1] Department of Physics and Astronomy, University College London, London WC1E 6BT, UK
[2] College of Science and Engineering, James Cook University, Townsville 4811, Australia

E-mail: `g.peach@ucl.ac.uk`

**Abstract.**
Photoassociation processes are studied in ultracold collisions between different isotopes of metastable He($2^3$S) and He($2^3$P) atoms; Penning and associative ionization rates for collisions between two He($2^3$S) atoms are also obtained. Comparisons are made with data from existing experiments.

## 1. Introduction

Bose-Einstein condensation (BEC) was first observed in alkali atoms in 1995 and a little later in atomic hydrogen. Initially condensates were all formed from atoms in their ground electronic states but subsequently, the search was on to obtain condensates of atoms in excited states. In 2001, a condensate was observed in a dilute gas of $^4$He($2^3$S) at a critical temperature of $4.5 \pm 0.5$ $\mu$K with a maximum number of condensed atoms of about 5 x $10^5$.
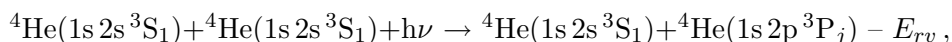
Ultracold collisions of metastable helium atoms are now widely used to study collision dynamics in dilute quantum gases as the large internal energy can be released during collisions, allowing novel experimental strategies based upon single atom detection to be implemented. Photoassociation of ultracold atoms provides a powerful technique for the study of ultracold collisions in which two interacting cold atoms are resonantly excited by a laser to bound states of the associated molecule. The resulting spectra have a very high resolution of < 1 MHz.

Currently we are investigating elastic and ionizing collisions in spin-polarized metastable helium in the absence of an exciting laser, where the spin-dipole interaction can induce relaxation from the initial spin-polarized state to states from which Penning and associative ionization is highly probable.

## 2. Theory

### 2.1. Photoassociation

Photoassociation of ultracold bosonic homonuclear metastable helium has been observed by many groups. The system $^4$He$^* + {}^4$He$^*$ is resonantly excited by a laser photon with energy h$\nu$ in the processes

$$^4\text{He}(1\text{s}\,2\text{s}\,^3\text{S}_1) + {}^4\text{He}(1\text{s}\,2\text{s}\,^3\text{S}_1) + \text{h}\nu \rightarrow {}^4\text{He}(1\text{s}\,2\text{s}\,^3\text{S}_1) + {}^4\text{He}(1\text{s}\,2\text{p}\,^3\text{P}_j) - E_{rv}\,,$$

where $j$=0,1,2 and $E_{rv}$ is the binding energy of the rovibrational bound state relative to the limit $^4$He($1\text{s}\,2\text{s}\,^3$S)$+{}^4$He($1\text{s}\,2\text{p}\,^3\text{P}_j$). These states occur in shallow potential wells at interatomic separations $\geq 150$ $a_0$. We have carried out detailed calculations for these processes [1] and have extended the theory to consider the similar systems $^3$He$^*+{}^3$He$^*$ [2] and $^3$He$^*+{}^4$He$^*$ [3].

**Table 1.** Helium: Energy levels in MHz

| $^4$He fine structure levels | $^3$He hyperfine structure levels |
|---|---|
| | $2^3P_0$ $f=\frac{1}{2}$ 34385.941 |
| 34061.912 $2^3P_0$ | |
| | $2^3P_2$ $f=\frac{3}{2}$ 6961.104 |
| 6462.553 $2^3P_1$ | |
| | $2^3P_1$ $f=\frac{1}{2}$ 6293.071 |
| 2153.072 $2^3P_2$ | |
| | $2^3P_1$ $f=\frac{3}{2}$ 1780.880 |
| | $2^3P_2$ $f=\frac{5}{2}$ 0 |
| | |
| | $2^3S_1$ $f=\frac{1}{2}$ 6739.701177 |
| 2246.567 $2^3S_1$ | |
| | $2^3S_1$ $f=\frac{3}{2}$ 0 |

Quite distinct results are obtained for the different isotope combinations because the hyperfine structure of the $^3$He states cannot be neglected. The relevant energy levels are shown in table 1.

The bound rovibrational levels of the ultracold excited metastable helium system are found by analyzing the eigenvalues of the molecular Hamiltonian

$$\hat{H} = \hat{T} + \hat{H}_{\rm rot} + \hat{H}_{\rm el} + \hat{H}_{\rm fs} + \hat{H}_{\rm hfs}\,,$$

where $\hat{T}$ is the kinetic energy operator

$$\hat{T} = -\frac{\hbar^2}{2\mu R^2}\frac{\partial}{\partial R}\left(R^2\frac{\partial}{\partial R}\right)\,,$$

and $\hat{H}_{\rm rot}$ is the rotational operator

$$\hat{H}_{\rm rot} = \frac{\hat{l}^2}{2\mu R^2}\,,$$

for a system of two atoms with interatomic separation $R$, reduced mass $\mu$ and relative angular momentum $\hat{\mathbf{l}}$.

The total electronic Hamiltonian is

$$\hat{H}_{\rm el} = \hat{H}_1 + \hat{H}_2 + \hat{H}_{12}\,,$$

where the unperturbed atoms have Hamiltonians $\hat{H}_i$, $i = 1, 2$ and their electrostatic interaction is specified by $\hat{H}_{12}$. The terms $\hat{H}_{\rm fs}$ and $\hat{H}_{\rm hfs}$ describe the fine and hyperfine structure of the atoms.

The multichannel equations describing the interacting atoms are obtained from the eigenvalue equation

$$\hat{H}|\Psi\rangle = E|\Psi\rangle$$

by expanding the eigenvector in terms of basis states in the form $|\Phi_a\rangle = |\Phi_a(R, q)\rangle$. Here, $a$ denotes the set of approximate quantum numbers describing the electronic-rotational states of the molecule and $q$ denotes the interatomic polar coordinates $(\theta, \phi)$ and electronic coordinates $(\mathbf{r}_1, \mathbf{r}_2)$.

The expansion

$$|\Psi\rangle = \sum_a \frac{1}{R} G_a(R) |\Phi_a\rangle$$

yields the multichannel equations

$$\sum_a \left\{ T_{a'a}^G(R) + \left[ V_{a'a}(R) - E\delta_{a'a} \right] G_a(R) \right\} = 0 \, ,$$

where

$$T_{a'a}^G(R) = -\frac{\hbar^2}{2\mu} \langle \Phi_{a'} | \frac{\partial^2}{\partial R^2} G_a(R) | \Phi_a \rangle$$

and

$$V_{a'a}(R) = \langle \Phi_{a'} | \left[ \hat{H}_{\mathrm{rot}} + \hat{H}_{\mathrm{el}} + \hat{H}_{\mathrm{fs}} + \hat{H}_{\mathrm{hfs}} \right] | \Phi_a \rangle \, .$$
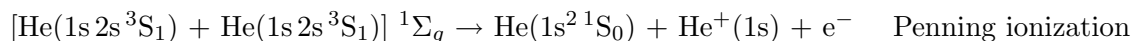
*2.2. Potentials*

The required Born-Oppenheimer potentials $^{1,3,5}\Sigma_{g,u}^+$ and $^{1,3,5}\Pi_{g,u}$, see [4], were constructed by matching *ab initio* MCSCF and MRCI short-range potentials onto the long-range dipole-dipole plus dispersion potentials given by

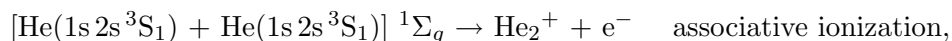$$V_\Lambda^{\mathrm{long}}(R) = -f_{3\Lambda}(R/\lambda)C_{3\Lambda}/R^3 - C_{6\Lambda}/R^6 - C_{8\Lambda}^\pm/R^8,$$

where $\Lambda = \Sigma, \Pi$ and $f_{3\Lambda}$ is an $R$- and $\Lambda$-dependent retardation correction. The wavelength for the transition $2\mathrm{s}\,^3\mathrm{S}$–$2\mathrm{p}\,^3\mathrm{P}$ is $\lambda$, where $\lambda/(2\pi) = 3258.17\, a_0$ and the superscripts indicate the sign of $(-1)^{S+w}$, $S = 0,1,2$, $w = 0$ or 1 (gerade/ungerade). The coefficients $C_{n\Lambda}$; $n = 3,6,8$ are well known, see [5] and [6].

*2.3. Scattering processes*

In the absence of an exciting laser, ionizing collisions in spin-polarized metastable helium can still take place because the spin-dipole interaction can induce relaxation from the initial spin-polarized state to spin states of $[\mathrm{He}(2\,^3\mathrm{S}_1) + \mathrm{He}(2\,^3\mathrm{S}_1)]$ from which Penning and associative ionization is highly probable. These processes are:

$$[\mathrm{He}(1\mathrm{s}\,2\mathrm{s}\,^3\mathrm{S}_1) + \mathrm{He}(1\mathrm{s}\,2\mathrm{s}\,^3\mathrm{S}_1)] \,^1\Sigma_g \rightarrow \mathrm{He}(1\mathrm{s}^2\,^1\mathrm{S}_0) + \mathrm{He}^+(1\mathrm{s}) + \mathrm{e}^- \quad \text{Penning ionization}$$

and

$$[\mathrm{He}(1\mathrm{s}\,2\mathrm{s}\,^3\mathrm{S}_1) + \mathrm{He}(1\mathrm{s}\,2\mathrm{s}\,^3\mathrm{S}_1)] \,^1\Sigma_g \rightarrow \mathrm{He}_2^+ + \mathrm{e}^- \quad \text{associative ionization,}$$

where if $[\mathrm{He}(1\mathrm{s}\,2\mathrm{s}\,^3\mathrm{S}_1) + \mathrm{He}(1\mathrm{s}\,2\mathrm{s}\,^3\mathrm{S}_1)]$ is prepared in the $\mathrm{He}_2\,^5\Sigma_g$ state the transition rate to the $\mathrm{He}_2\,^1\Sigma_g$ state is small. If this transition does take place, Penning ionization or associative ionization follows rapidly leaving the helium atoms/molecules in their ground electronic states. The collisions between isotopes $^4\mathrm{He}$ and $^3\mathrm{He}$ are being studied for all three combinations, 4-4, 3-3 and 3-4.

We consider the relative motion of the atoms subject to a central interatomic potential $V(R)$ where

$$V(R) = V_0(R) + V_{\text{ion}}(R)$$

and $V_0(R)$ is the adiabatic potential for the $^1\Sigma_g$ state of the He$^*$+He$^*$ system. The potential $V_{\text{ion}}(R)$ is included to allow for loss processes. Two ionization models are used, M1 and M2, see [7] and $V_0(R)$ is determined from experimental and theoretical data [8], [9] and [10].

The two models are specified by

$$(M1) \qquad V_{\text{ion}}(R) = +\infty\,; \quad R \le R_b$$
$$= \quad 0\,; \quad R > R_b$$

and

$$(M2) \qquad V_{\text{ion}}(R) = -\frac{1}{2}i\,\Gamma(R);\quad \Gamma(R) = 0.3a_0 \exp(-R/1.086a_0)\,.$$

In both cases on integrating the radial wave equation we obtain a $2\times 2$ scattering matrix $S$ which must be unitary and symmetric. The cross sections $\sigma(v)$ as a function of the relative velocity $v$ are given by

$$\sigma_{\text{elastic}}(v) = \frac{\pi}{k^2} \sum (2l+1)|1 - S_{00}|^2\,; \quad \sigma_{\text{ionization}}(v) = \frac{\pi}{k^2} \sum (2l+1)|S_{01}|^2,$$

where $k = \mu v/\hbar$ and the rates $K_e$ and $K_i$ are obtained by averaging over a Maxwell velocity distribution so that

$$K_e = [v\sigma_{\text{elastic}}(v)]_{\text{av}}; \quad K_i = [v\sigma_{\text{ionization}}(v)]_{\text{av}}\,.$$

The sum $\sum$ over the angular momentum quantum number $l$ for the heteronuclear system $^3$He $+$ $^4$He is taken over all values of $l$, but the systems $^4$He $+$ $^4$He and $^3$He $+$ $^3$He are symmetric and anti-symmetric respectively with respect to the interchange of the nuclear space and spin coordinates. This means that the sum $\sum$ has to be interpreted as

$$\sum \equiv 2 \sum_{l\,even}$$

for the bosonic case and

$$\sum \equiv \frac{1}{2} \sum_{l\,even} + \frac{3}{2} \sum_{l\,odd}$$

for the fermionic system.

The multichannel calculations include magnetic-dipole mediated transitions from the $^5\Sigma$ state and represent the ionization loss from the $^{1,3}\Sigma$ states by a complex optical potential. The asymptotic solutions of the multichannel equations yield the non-unitary scattering matrix elements $S_{a'a}$. The elastic cross section for channel $a$ is then

$$\sigma(a \to a; v) = \frac{\pi}{k^2} \sum (\ldots)|1 - S_{aa}|^2.$$

The ionization cross section is

$$\sigma(a \to \text{ion}; v) = \frac{\pi}{k^2} \sum (\ldots)|1 - S(a \to \text{ion})|^2$$

where $S(a \to \text{ion})$ is obtained from the non-unitarity of the $S$-matrix:

$$|S(a \to \text{ion})|^2 = 1 - \sum_{a'} |S_{a'a}|^2.$$

In the above $\sum(\ldots)$ denotes sum/average over unobserved quantum numbers.

**Table 2.** $^4$He($2^3$S)+$^4$He($2^3$P). Photoassociation
Energies in GHz relative to the $j = 2$ asymptote. The third column lists the levels after a 1% variation is applied to the short-range potentials.

| Exp | Theor | Variation | assignment |
|--------|---------|-----------|-----------------------|
| -13.57 | -13.259 | -13.621 | $2_u,\ J = 3$ |
| -11.70 | -11.434 | -11.764 | $1_u,\ J = 1$ |
| -11.10 | -10.930 | -11.224 | $1_u, 0_u^+\ J = 3$ |
| -8.94 | -8.705 | -8.966 | $2_u,\ J = 3$ |
| -7.44 | -7.262 | -7.493 | $1_u,\ J = 1$ |
| -7.01 | | -7.103 | $1_u, 0_u^+\ J = 3$ |
| -5.64 | -5.463 | -5.647 | $2_u,\ J = 3$ |
| -4.53 | -4.394 | -4.551 | $1_u, 0_u^+,\ J = 1$ |
| -4.26 | -4.145 | -4.285 | $0_u^+, 1_u,\ J = 3$ |
| -3.49 | -3.438 | -3.566 | $2_u,\ J = 2$ |
| -3.38 | -3.251 | -3.375 | $2_u,\ J = 3$ |

## 3. Results

### 3.1. Photoassociation

Three sets of calculations have been undertaken: single-channel, multichannel without Coriolis couplings and full multichannel with Coriolis couplings. At each value of $R$ the single-channel potential is formed by diagonalizing the matrix:

$$V_{a'a}^{\Omega_j} = \langle a'|\hat{H}_{\text{el}}|a\rangle + \langle a'|\hat{H}_{\text{fs}} + \hat{H}_{\text{hfs}}|a\rangle + \frac{\langle a'|\hat{l}^2|a\rangle_{\Omega_j}}{2\mu R^2},$$

where $\langle a'|\hat{l}^2|a\rangle_{\Omega_j}$ is the part of $\langle a'|\hat{l}^2|a\rangle$ diagonal in $\Omega_j$. $\Omega_j$ denotes the projection of the total angular momentum quantum number $J$ onto the inter-molecular axis. Results shown in table 2 illustrate the excellent agreement beteen theory and experiment that can be achieved. More details are given in [1].

### 3.2. Scattering processes

Rates $K_e$ and $K_i$ as a function of temperature $T$ for the elastic scattering and ionization processes obtained using models M1 (with $R_b = 7a_0$) and M2 are listed in table 3, where Model M1 is insensitive to the precise choice of $R_b$.

The results from the two models agree quite well with each other and show that the rates become increasingly insensitive to the form of $V_{\text{ion}}(R)$ as the temperature increases. In table 4 total unpolarized ionization rates are listed for combinations of the different isotopes of helium, where allowance is made for contributions from all the initial spin states of He($2^3$S)+He($2^3$S), $^1\Sigma_g$, $^3\Sigma_u$ and $^5\Sigma_g$.

Full quantum-mechanical close-coupled calculations are also being carried out and provisional results $K$(theor) see [11], agree quite well with those of a simple two-stage semi-classical model $K$(sc) and with experiment $K$(exp), see [12] and [13].

## 4. Conclusions

Our analysis of photoassociation processes in the $^4$He$^*$+$^4$He$^*$ system, based upon single-channel and multichannel calculations, permitted criteria to be established for the assignment of the

**Table 3.** $^4$He($2^3$S)$+^4$He($2^3$S). Scattering

The elastic ($K_e$) and ionization ($K_i$) rates for models M1 and M2 are in units of cm$^3$/s and the data are listed in the form $4.914(-12) = 4.914\times 10^{-12}$.

| $\text{Log}_{10}(T(\text{K}))$ | $K_e(\text{M1})$ | $K_e(\text{M2})$ | $K_i(\text{M1})$ | $K_i(\text{M2})$ |
|---|---|---|---|---|
| -7.0 | 4.914(-12) | 4.216(-12) | 1.329 (-9) | 1.277 (-9) |
| -6.0 | 1.540(-11) | 1.322(-11) | 1.319 (-9) | 1.268 (-9) |
| -5.0 | 4.739(-11) | 4.072(-11) | 1.289 (-9) | 1.239 (-9) |
| -4.0 | 1.374(-10) | 1.185(-10) | 1.198 (-9) | 1.155 (-9) |
| -3.0 | 3.324(-10) | 2.895(-10) | 9.663(-10) | 9.367(-10) |
| -2.0 | 5.066(-10) | 4.615(-10) | 6.980(-10) | 6.836(-10) |
| -1.0 | 7.424(-10) | 7.152(-10) | 1.066 (-9) | 1.028 (-9) |
| 0.0 | 1.720 (-9) | 1.712 (-9) | 1.567 (-9) | 1.601 (-9) |

**Table 4.** He($2^3$S)$+$He($2^3$S). Scattering

Thermally averaged total unpolarized ionization rates $K$ for the 3-3, 3-4 and 4-4 systems in units of cm$^3$/s.

| System | $T(\text{mK})$ | $K(\text{exp})$ | $K(\text{theor})$ | $K(\text{sc})$ |
|---|---|---|---|---|
| 4-4 | 1.9(1) | 8(2) $\times 10^{-11}$ | $9.74\times 10^{-11}$ | $8.0\times 10^{-11}$ |
| 3-3 | 2.0(3) | $1.8(3)\times 10^{-10}$ | $1.30\times 10^{-10}$ | $1.7\times 10^{-10}$ |
| 3-4 | 1.2(1) | $2.5(8)\times 10^{-10}$ | $2.42\times 10^{-10}$ | $2.4\times 10^{-10}$ |

theoretical levels to the experimental observations. Excellent agreement was obtained for the nearly 50 observed levels. We have also investigated photoassociation in the fermionic metastable homonuclear $^3$He*$+^3$He* system, where the hyperfine structure leads to a very different pattern of energy levels below the $^3$He($1s\,2s\,^3$S)$+^3$He($1s\,2p\,^3$P$_j$) asymptotes. As no experimental observations are available for this system, we have assessed the observability of the theoretical levels and have identified purely long-range levels and 30 short-range levels suitable for experimental investigation. Very recently we have extended our investigations to photoassociation in the heteronuclear $^3$He*$+^4$He* system. No purely bound long-range states were found, although several resonances with line widths smaller than 1 MHz were obtained.

Currently we are investigating elastic and ionizing collisions in spin-polarized metastable $^4$He*$+^4$He*, $^3$He*$+^3$He* and $^3$He*$+^4$He* systems in the absence of an exciting laser, where the spin-dipole interaction can induce relaxation from the initial spin-polarized state to states from which Penning and associative ionization is highly probable. Two simple models are adopted from which rates for elastic scattering and ionization processes have been calculated for the $^4$He*$+^4$He* system. The results from the two models agree quite well with each other, and preliminary results from full solutions of the quantum-mechanical coupled equations indicate that the simple models give a good general description of the process.

**References**

[1] Cocks D G, Whittingham I B and Peach G 2010 *J. Phys.* B: *At. Mol. Opt. Phys.* **43** 135102
[2] Cocks D G, Peach G and Whittingham I B 2011 *Phys. Chem. Chem. Phys.* **13** 18724–33
[3] Peach G, Cocks D G and Whittingham I B 2015 *J. Phys.* B: *At. Mol. Opt. Phys.* **48** 115205

[4]  Deguilhem B, Leininger T, Gadéa F X and Dickinson A S 2009 *J. Phys.* B: At. Mol. Opt. Phys. **42** 015102
[5]  Venturi V, Leo P J, Tiesinga E, Williams C J and Whittingham I B 2003 *Phys. Rev.* A **68** 022706
[6]  Zhang J-Y, Yan Z-C, Vrinceanu D, Babb J F and Sadeghour H R 2006 *Phys. Rev.* A **73** 022710
[7]  Garrison B J, Miller W H and Schaefer H F 1973 *J. Chem. Phys.* **59** 3193
[8]  Müller M W, Merz A, Ruf M-W, Hotop H, Meyer W and Movre M 1991 *Z. Phys.* D: At. Mol. Clusters **21** 89-112
[9]  Stärck T and Meyer W 1994 *Chem. Phys. Lett.* **225** 229
[10]  Venturi V and Whittingham I B 2000 *Phys. Rev.* A **61** 060703(R)
[11]  Cocks D G, Whittingham I B and Peach G (to be published)
[12]  Stas R J W, McNamara J M, Hogervorst W and Vassen W 2006 *Phys. Rev.* A **73** 032713
[13]  McNamara J M, Stas R J W, Hogervorst W and Vassen W 2007 *Phys. Rev.* A **75** 062715